Electronic structure and anisotropic transport properties in hexagonal YPtIn and LuAgGe ternary compounds

2006 J. Phys.: Condens. Matter 18 1473

(http://iopscience.iop.org/0953-8984/18/4/030)

INSTITUTE OF PHYSICS PUBLISHING JOURNAL OF PHYSICS: CONDENSED MATTER

J. Phys.: Condens. Matter **18** (2006) 1473–1482 doi:10.1088/0953-8984/18/4/030

Electronic structure and anisotropic transport properties in hexagonal YPtIn and LuAgGe ternary compounds

G D Samolyuk, S L Bud'ko, E Morosan, V P Antropov and P C Canfield

Ames Laboratory US DOE and Department of Physics and Astronomy, Iowa State University, Ames, IA 50011, USA

Received 14 August 2005
Published 13 January 2006
Online at stacks.iop.org/JPhysCM/18/1473

Abstract

We present anisotropic, zero applied magnetic field, temperature-dependent resistivity measurements on hexagonal, non-magnetic YPtIn and LuAgGe single crystals. For these materials the in-plane resistivity, ρ_{ab}, is significantly higher than the c-axis one, ρ_c, with $\rho_{ab}/\rho_c \approx 1.4$ for YPtIn and ≈4.2–4.7 for LuAgGe. The connection between the electronic structure and the anisotropic transport properties is discussed using density functional calculations that link the observed anisotropy with a specific shape of Fermi surface and anisotropy of the Fermi velocities.

(Some figures in this article are in colour only in the electronic version)

1. Introduction

Interest in the RAgGe and RPtIn (R = rare earth) ternary intermetallics [1, 2] was recently stimulated by the growth of single crystals of these materials and in-depth characterization of their thermodynamic and transport properties [3, 4]. Due to the curious combination of crystallographic (hexagonal) and point (orthorhombic) symmetries of the rare earths in these two families, local magnetic moment members of the series have complex (but tractable) anisotropic H–T phase diagrams, with intriguing metamagnetism as well as crystal electric field effects playing a significant role in defining the magnetic order [4, 5]. YbAgGe and YbPtIn have been described as heavy fermion compounds [3, 6–8] with YbAgGe being a rare example of a Yb-based stoichiometric compound demonstrating field-induced non-Fermi-liquid behaviour [9, 10]. YbPtIn displays similar properties but with a less comprehensively determined phase diagram [11].

The non-magnetic members of these families, LuAgGe and YPtIn, have rather unpretentious physical properties [3, 4]; however, understanding of these materials from the band-structure point of view can be viewed as the first step towards comprehension of the rest of the series, especially since they serve as non-magnetic references in the analysis of the

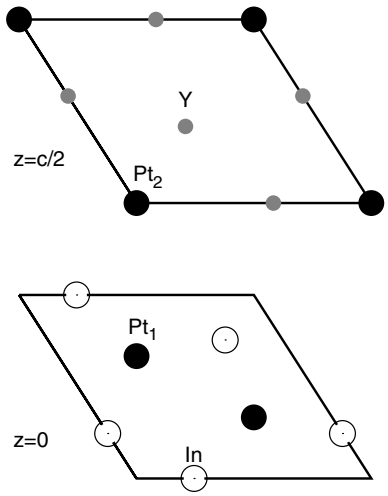

Figure 1. The unit cell of YPtIn (hexagonal structure of ZrNiAl-type).

physical properties across the series. In particular, the anisotropic crystal structure suggests measurable anisotropy of the transport properties. Comparison of the experimental resistivity data with computational band-structure results will serve as a test of the theoretical description of these materials and will allow for the identification of the qualitative features of their Fermi surfaces responsible for the anisotropy.

2. Experimental methods and computational details

LuAgGe and YPtIn single crystals in the form of rods of several millimetres in length with a hexagonal-cross-section of up to 1 mm^2 were grown from high-temperature ternary solutions (rich in Ag and Ge for LuAgGe and in In for YPtIn); their structure and the absence of impurity phases were confirmed by powder x-ray diffraction (see [3, 11] for details of the samples' growth and characterization). For resistivity measurements with $I \parallel c$, clean, regular-shaped as-grown or lightly polished rods were used. Samples for $I \parallel ab$ measurements were cut out of thicker rods, with their length approximately along the [110] crystallographic direction. In the case of YPtIn particular care was taken to eliminate residues of highly conductive In flux (by polishing with subsequent etching in HCl) that otherwise could affect the current flowing through the sample (i.e. practically shorting out the sample) resulting in erroneous values for resistivity and its temperature dependence. The absence of any anomaly in resistivity near $T_c^{In} = 3.4$ K served as an indication of a clean sample.

Resistivity measurements were performed over the 2–300 K temperature range in standard four-probe configuration with thin platinum wires attached to the samples by Epotek H20E silver epoxy, using the ACT option of the Quantum Design PPMS instrument ($f = 16$ Hz, $I = 1$–3 mA). For each direction of the current several samples were used and the results were within the error bars ($\sim$20%) of the measurements of the dimensions of the samples and the position of the voltage leads.

Both LuAgGe [1] and YPtIn [2] crystallize in a Fe_2P/ZrNiAl-type of structure ($P62m$ space group) with nine atoms per unit cell (figure 1). The $z = 0$ plane is occupied by Pt(Ge), In(Ag) atoms, whereas the $z = c/2$ plane contains Y(Lu), Pt(Ge) atoms. The apparent layered character of this structure may lead to strong anisotropy of the Fermi surface.

The electronic structure was calculated using the atomic sphere approximation tight-binding linear muffin-tin orbital (TB-LMTO-ASA) method [12, 13] within the local density approximation (LDA) with Barth–Hedin [14] exchange–correlation at experimental values of the lattice parameters. A mesh of 4699 $\vec{k}$ points in the irreducible part of the Brillouin zone (BZ) was sufficient to reach a few per cent accuracy in the calculated conductivity tensor. 3d electrons of Ge and 4d electrons of In were included in the core states. 4f electrons of the Lu atom were treated as the valence states.

With the purpose of investigating the anisotropic behaviour of transport properties, we implement the expression for diffusion conductivity in the relaxation time approximation [15]:

$$\sigma_\alpha(E) \propto \tau \sum_{\vec{k},\nu} v_\nu^\alpha(\vec{k}) v_\nu^\alpha(\vec{k}) \delta[\varepsilon_\nu(\vec{k}) - E] \equiv \tau \langle v^\alpha v^\alpha \rangle. \tag{1}$$

In equation (1), τ is the relaxation time, $v_\nu^\alpha = \partial\varepsilon_\nu(\vec{k})/\partial\vec{k}$ is the electronic group velocity, $\varepsilon_\nu(\vec{k})$ is the energy spectrum, $\vec{k}$ and ν are the wavevector and band index and E corresponds to Fermi energy (E_F).

3. Results and discussion

3.1. Experiment

Zero-field resistivity data for different directions of the current flow in LuAgGe and YPtIn are shown in figure 2. For both materials $\rho_{ab} < \rho_c$, although in both cases the normalized resistivities (see insets to figures 2(a),(b)) are practically isotropic. This observation (the coincidence of the normalized in-plane and axial resistivities) is consistent with the conjecture that the anisotropy in resistivity is dominated by the anisotropy in the Fermi velocity with the relaxation time, τ, being the same for different directions of the current flow. The measured anisotropy in resistivity at 300 K is 4.2 (LuAgGe) and 1.4 (YPtIn). It should be noted that, given the aforementioned (conservative) estimate of the error bars for the absolute values of resistivity, the $\rho(T)$ for YPtIn may be close to being isotropic whereas for LuAgGe the inequality $\rho_{ab} < \rho_c$ is unambiguous. The residual resistivity ratios (RRR) are quite low, 1.5–2; similarly mediocre RRR were observed for the other members of these families [3, 4]. The absolute values of the residual resistivities appear to be higher that usually seen in intermetallic compounds, suggesting possible defects and/or site disorder in the crystals on the levels below the powder x-ray diffraction resolution. Another possible contribution to the high resistivity values will be discussed in section 3.2. Anisotropic susceptibility and electronic coefficient of the specific heat of these two materials were reported earlier [3, 4]. For LuAgGe $\chi_{ab}(300\ \mathrm{K}) \approx -3.3 \times 10^{-5}$ emu mol^{-1}, $\chi_c(300\ \mathrm{K}) \approx -5 \times 10^{-5}$ emu mol^{-1}, $\gamma \approx 1.4$ mJ mol^{-1} K^{-2}; for YPtIn $\chi_{ab}(300\ \mathrm{K}) \approx 6.6 \times 10^{-5}$ emu mol^{-1}, $\chi_c(300\ \mathrm{K}) \approx 4.6 \times 10^{-5}$ emu mol^{-1}, $\gamma \approx 6.7$ mJ mol^{-1} K^{-2}. The magnetic susceptibility for both compounds is slightly anisotropic and on a gross level it is temperature independent (except for the small, low-temperature impurity tail). Since it is quite difficult to quantitatively account for different contributions to susceptibility (Landau, core, etc) (see e.g. [16]) we will not attempt to compare the measured values with the band structure calculations. The electronic coefficient of the specific heat, γ, on the other hand, can be useful for evaluating the band structure calculations.

3.2. Electronic structure

The calculated total and partial densities of states (DOS) for YPtIn are shown in figure 3. The sharp peak at -6.5 eV below the Fermi level (E_F) corresponds to In s-bands (figure 4). These

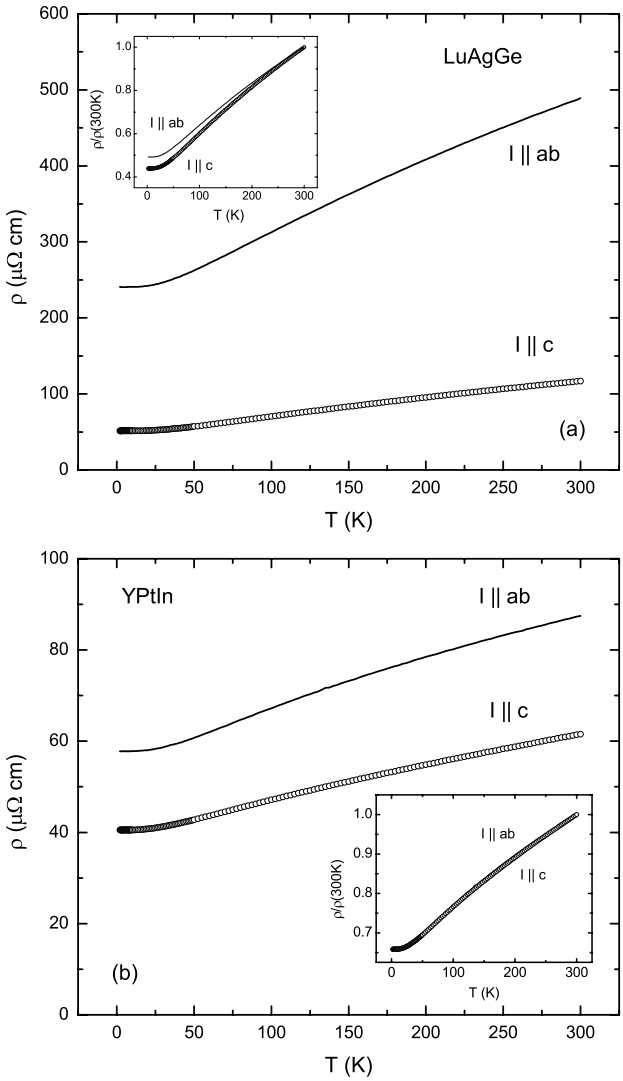

Figure 2. Anisotropic zero-field resistivity of (a) LuAgGe and (b) YPtIn. Insets: the same data normalized to $\rho(300\ \mathrm{K})$.

states are strongly hybridized with s-states of Pt atoms. A gap of 0.4 eV separates the In and Pt s-states from the conductivity electron band. The Pt d-states are localized at −4 eV and are hybridized with d-states of Y and p-states of In atoms. At E_F the contribution of the electrons originating from all atoms is nearly the same and is proportional to the number of corresponding atoms in the unit cell. The electronic specific heat coefficient γ_{band} calculated from DOS at E_F ($N(E_F)$) (table 1) is 4.2 mJ mol^{-1} K^{-2}.

In the LuAgGe compound the Ge s-state band is separated from the conductivity electron band by a 2 eV gap (figures 5 and 6). This value is significantly larger than that for YPtIn. The difference in the gap size is due to the deeper position of the Ge s-electrons states than in In and the smaller width of the d-band in 4d- compared with 5d-metals [17]. The Lu 4f-states are located around 5 eV below E_F within the range of the Ag d-states and they show a very

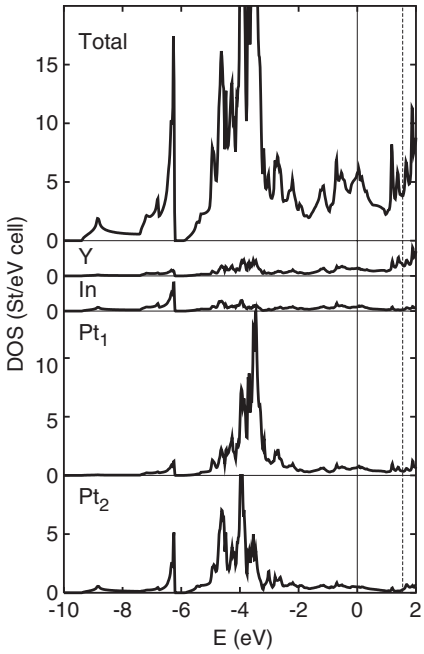

Figure 3. The total and partial DOS for the YPtIn. E_F corresponds to zero energy (the unit cell contains 48 valence electrons). The energy, which corresponds to 54 valence electrons in a unit cell (number of valence electrons for LuAgGe without Lu f-electrons) is shown by the dashed line. The vertical scales are the same for all panels.

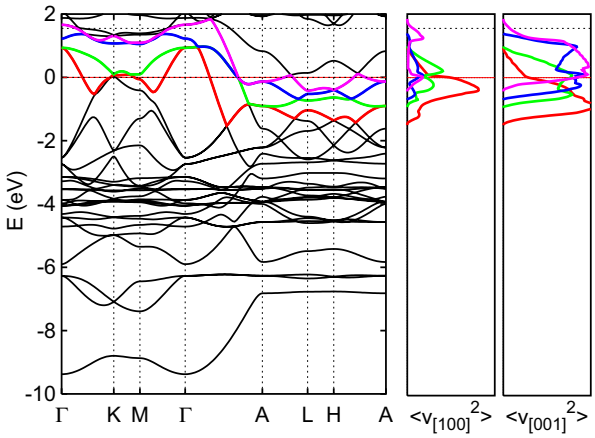

Figure 4. The band structure (left panel) and [100], [001] components of the velocity tensor as a function of energy (right panels) for YPtIn. E_F corresponds to zero energy (the unit cell contains 48 valence electrons). The E_F, which corresponds to 54 valence electrons, is shown by the horizontal dashed line.

little dispersion. In contrast to YPtIn the E_F in LuAgGe compound is placed in a pseudo-gap. The $N(E_F)$ equals 1.92 states/(Ryd atom). This decrease of $N(E_F)$ translates into a four times smaller γ_{band} value compared with YPtIn (table 1). The main contribution to $N(E_F)$ comes from the d-states of Lu and the p-states of Ge1 atoms located in the same plane as Lu.

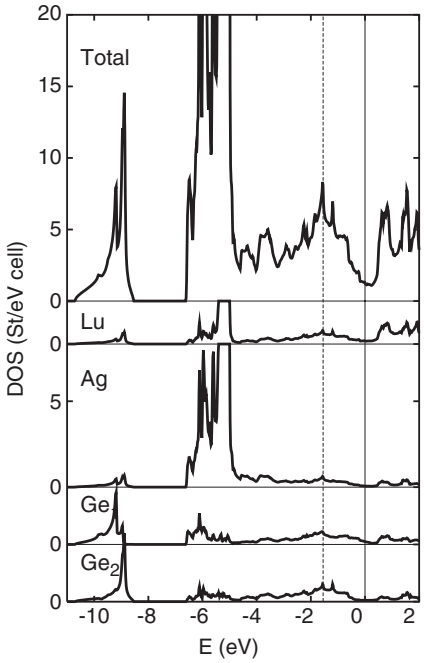

Figure 5. The total and partial DOS for the compound LuAgGe. E_F corresponds to zero energy (the unit cell contains 96 valence electrons). The E_F, which corresponds to 90 valence electrons, is shown by the vertical dashed line.

Table 1. Experimental lattice constants in Å, DOS in states/(Ryd atom), electronic specific heat coefficient in mJ mol^{-1} K^{-2} and conductivity anisotropy.

				γ		$\frac{\langle v^2_{[001]}\rangle}{\langle v^2_{[100]}\rangle}$	
Compound	a	c	DOS	Calc.	Exp.	Calc.	Exp.
YPtIn	7.583	3.846	8.17	4.2	6.7	2.7	1.4
LuAgGe	7.027	4.127	1.92	1.0	1.4	3.2	4.2

The comparison of the calculated, γ_{band}, and measured, γ_{exp}, electronic specific heat coefficients (table 1) as $\gamma_{exp} = \gamma_{band}(1 + \lambda)$ give a value of the enhancement factor λ (due to the electron–electron and electron–phonon interactions) of 0.4–0.6. Such λ values are very common for ordinary metals and were observed, for example, for several alkali metals [18], being attributed mainly to the electron–phonon interactions.

To demonstrate the similarity of the electronic structures for YPtIn and LuAgGe we calculated the E_F position using the YPtIn DOS for 54 valence electrons per unit cell (this number of electrons corresponds to the LuAgGe compound without Lu 4f-states) (see vertical dashed line in figure 3). The obtained E_F equals 1.8 eV and is placed very close to the pseudo-gap in the DOS. The E_F calculated from the LuAgGe DOS (figure 5) for 90 electrons per cell (this number of electrons corresponds to hypothetical compound with 48 electrons from YPtIn ligands plus additional $3 \times 14 = 42$ f-electrons from the rare earth) equals -1.8 eV and is placed at the peak in DOS very similar to the one in YPtIn. These results suggest that the

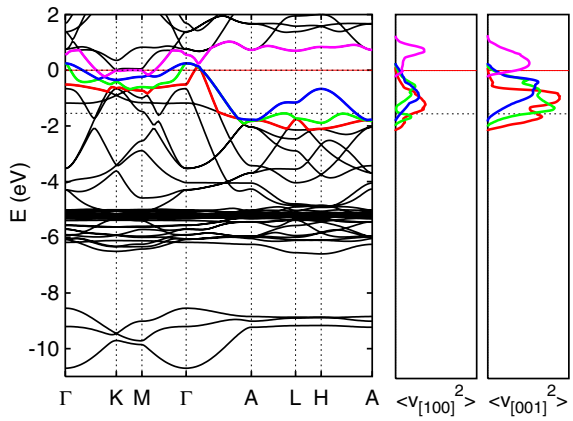

Figure 6. The band structure (left panel) and [100], [001] components of the velocity tensor as a function of energy (right panels) for LuAgGe. E_F corresponds to zero energy (the unit cell contains 96 valence electrons). The E_F, which corresponds to 90 valence electrons, is shown by the horizontal dashed line.

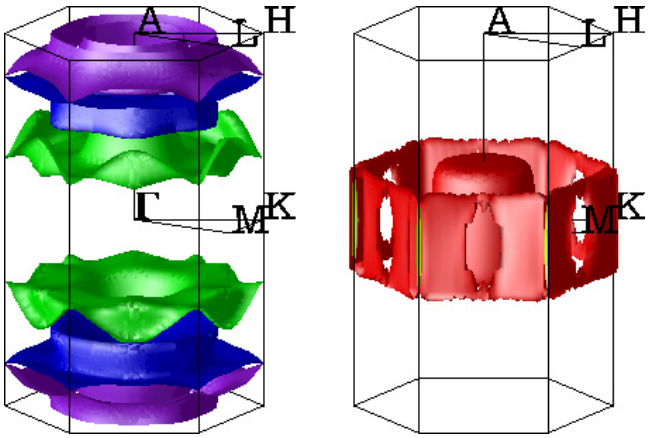

Figure 7. The Fermi surface of YPtIn. The colours of the different sheets (in the electronic version) correspond to the band colours in figure 4.

rigid-band approximation could be a reasonable approach for the analysis of the conductivity as a function of the band filling.

The partial contributions from the different bands to the velocity tensor $\langle v^\alpha v^\alpha \rangle$ for the in-plane direction ([100]) and perpendicular to the plane direction ([001]) are shown in the left panels of figures 4 and 6. The sizable difference between the velocity tensor in [001] and [100] directions is caused by larger dispersion of bands crossing the Fermi level in the Γ–A direction compared with Γ–K. Whereas it is difficult to single out the band responsible for the conductivity anisotropy in YPtIn, for LuAgGe it is the Lu d-band and the Ge1 p-band (shown in purple in the electronic version of figure 6).

This anisotropy of the Fermi velocity distribution is caused by a mainly two-dimensional shape of the Fermi surface (FS) of YPtIn (the Fermi velocity is perpendicular to the Fermi surface) (figure 7). At least two of the four FS sheets are open quasi-two-dimensional surfaces perpendicular to the [001] direction. Such a shape of the FS sheets is in turn determined by

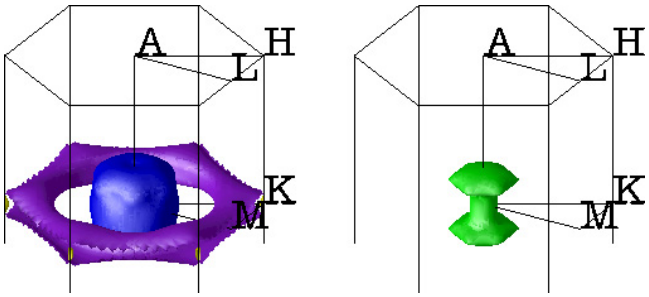

Figure 8. The Fermi surface of LuAgGe. The colours of the different sheets (in the electronic version) correspond to the band colours in figure 6. Two (red c.f. figure 6 in the electronic version) strawberry-shaped Fermi surface sheets centred near the centres of the dumbbell's discs are not shown.

the layered character of YPtIn, where layers of Y-Pt2 atoms are separated by layers of In-Pt2 atoms.

The FS of LuAgGe (figure 8) is somewhat different; however, the open quasi-two-dimensional character of one FS sheet is present for this material as well. This FS sheet is shown in purple in figure 8 and, as seen from figure 6 its contribution determines the anisotropic character of conductivity in LuAgGe.

The topology of the Fermi surfaces calculated for YPtIn and LuAgGe (figures 7, 8) suggests that the search for quantum oscillations in these materials may be rather complicated. Besides tiny needles centred at the K-point (in both materials), whose existence may be questionable because of numerical uncertainties, there are the Γ-centred dumbbell-shaped pockets (in LuAgGe) and the Γ-centred hassock- (marshmallow-)shaped pockets in both materials which may serve as possible candidates for de Haas–van Alphen/Shubnikov–de Haas studies. In addition, these pockets (as well as the quasi-two-dimensional sheets in YPtIn) might be studied separately if FS nesting features are analysed.

The dependency of the [100] and [001] components of the $\langle v^\alpha v^\alpha \rangle$ tensor as a function of band filling is shown in figure 9. The zero energy on these figures corresponds to occupation of 48 electrons calculated from the YPtIn DOS (bottom panel) and 48 plus 3 sets of 14 f-electrons for LuAgGe (top panel). The variation of the velocity tensors as a function of population in both these compounds is very similar. The mentioned applicability of the rigid band approximation allows us to predict (at least qualitatively) the increase (decrease) of conductivity anisotropy in YPtIn with substitution of Pt or In atoms by atoms with a larger (smaller) number of valence electrons. The resistivity anisotropy estimated from the calculated $\langle v^\alpha v^\alpha \rangle$ tensor is in reasonable agreement with experiment: $\rho_{ab} < \rho_c$ with LuAgGe being somewhat more anisotropic than YPtIn (table 1).

Finally, it is worth mentioning that the calculated values of the anisotropic average Fermi velocities for YPtIn and LuAgGe are rather small: the values for LuAgGe $v^x = \langle v^x v^x \rangle^{1/2} \approx 0.15 \times 10^8$ cm s^{-1}, $v^z = \langle v^z v^z \rangle^{1/2} \approx 0.25 \times 10^8$ cm s^{-1} are, for example, 7.4 and 4.4 times, respectively, lower than the average Fermi velocities, $v^{\langle 100 \rangle} \approx v^{\langle 110 \rangle} \approx 1.11 \times 10^8$ cm s^{-1}, for copper [19]. These low values of the Fermi velocities give an additional contribution to the observed high resistivities of YPtIn and LuAgGe. The mean free path, estimated from the residual resistivity and the respective average Fermi velocity, is, in the 'worst case' of ρ_{ab} of LuAgGe, more than four times larger than the unit cell dimensions, i.e. eight to nine times larger than the interatomic distances, that is consistent with the experimentally observed metallic ($\mathrm{d}\rho/\mathrm{d}T < 0$) behaviour of resistivity.

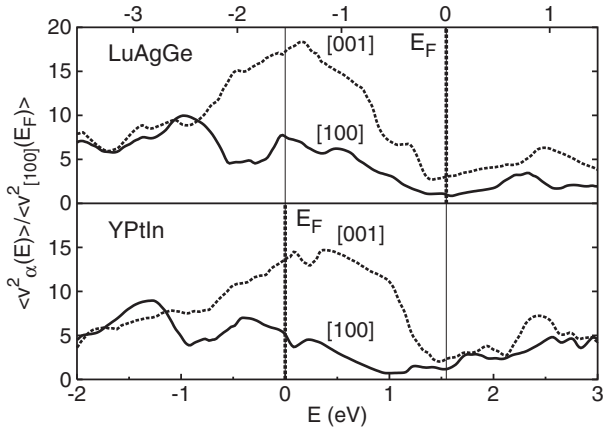

Figure 9. [100], [001] components of the Fermi velocities tensor as a function of E_F in YPtIn and LuAgGe compounds. E_F is shown by the vertical dashed line. The position of zero energy is explained in the text.

4. Summary

The electronic structure and transport properties were calculated and measured in YPtIn and LuAgGe compounds. The calculated electronic specific heat coefficient and conductivity anisotropy are in semi-quantitative agreement with experiment. It was shown that the observed anisotropy is a consequence of the shape of the Fermi surfaces of these compounds. In addition, the applicability of the rigid band approximation to describe the dependence of the conductivity anisotropy on non-isoelectronic doping is established. The calculated Fermi surfaces of YPtIn and LuAgGe can also be used for future measurements of photoemission and quantum oscillation and other properties of RPtIn and RAgGe (R = rare earth) series. Finally, we can infer from this work that the Fermi surface topology of the neighbouring (related) members of the RPtIn and RAgGe series will manifest a similar complexity.

Acknowledgments

Ames Laboratory is operated for the US Department of Energy by Iowa State University under contract no W-7405-Eng.-82. This work was supported by the director for Energy Research, Office of Basic Energy Sciences. One of the authors (GDS) would like to thank V G Kogan for enlightening discussions.

References

[1] Gibson B, Poettgen R, Kremer R K, Simon A and Ziebeck K R A 1996 *J. Alloys Compounds* **239** 34
[2] Ferro R, Marazza R and Rambaldi G 1974 *Z. Anorg. Allg. Chem.* **410** 219
[3] Morosan E, Bud'ko S L, Canfield P C, Torikachvili M S and Lacerda A H 2004 *J. Magn. Magn. Mater.* **227** 298
[4] Morosan E, Bud'ko S L and Canfield P C 2005 *Phys. Rev.* B **72** 014425
[5] Morosan E, Bud'ko S L and Canfield P C 2005 *Phys. Rev.* B **71** 014445
[6] Katoh K, Mano Y, Nakano K, Terui G, Niide Y and Ochiai A 2004 *J. Magn. Magn. Mater.* **268** 212
[7] Trovarelli O, Geibel C, Cardoso R, Mederle S, Borth R, Buschinger B, Grosche F M, Grin Y, Sparn G and Steglich F 2000 *Phys. Rev.* B **61** 9467
[8] Kaczorowski D, Andraka B, Pietri R, Cichorek T and Zaremba V I 2000 *Phys. Rev.* B **61** 15255
[9] Bud'ko S L, Morosan E and Canfield P C 2004 *Phys. Rev.* B **69** 014415

[10] Bud'ko S L, Morosan E and Canfield P C 2005 *Phys. Rev.* B **71** 054408
[11] Morosan E, Bud'ko S L, Mozharivskyj Yu and Canfield P C 2005 *Preprint* cond-mat/0506425
[12] Andersen O K 1975 *Phys. Rev.* B **12** 3060
[13] Andersen O K and Jepsen O 1984 *Phys. Rev. Lett.* **53** 2571
[14] von Barth A and Hedin L 1972 *J. Phys. C: Solid State Phys.* **5** 1629
[15] Ziman J M 1967 *Electrons and Phonons* (London: Oxford University Press)
[16] Schnelle W, Poettgen R, Kremer R K, Gmelin E and Jepsen O 1997 *J. Phys.: Condens. Matter* **9** 1435
[17] Andersen O K 1970 *Phys. Rev.* B **2** 883
[18] Grimvall G 1981 *The Electron–Phonon Interaction in Metals* (Amsterdam: North-Holland)
[19] Lee M J G 1970 *Phys. Rev.* B **2** 250